

Passivity-based control for maximum power extraction of thermoelectric generator

¹Abdelkader BELBOULA, ²Rachid TALEB, ¹Ghalem BACHIR

¹Electrical Engineering Department, University of Science and Technology of Oran-Mohamed Boudiaf (USTO-MB)
Laboratoire de Développement des Entraînements Electriques (LDEE), Oran, Algeria
aek.belboula@gmail.com

²Electrical Engineering Department, Hassiba Benbouali University
Laboratoire Génie Electrique et Energies Renouvelables (LGEER), Chlef, Algeria
rac.taleb@yahoo.fr

Abstract: *New robust algorithm of Maximum Power Point Tracking (MPPT) for an extraction system solar energy by thermoelectric effect is tackled in this paper. Indeed, the algorithms available today, suffer from non-robustness against climate change as well as system settings. This requires a deep study of the simulation of a robust controller system. Therefore, it is proposed, the Interconnection and Damping Assignment Passivity Based Control (IDA-PBC) application for maximum power point tracking (MPPT) of Thermoelectric Power Generator, which shows its efficiency and robustness compared to other methods (such as Incremental Conduction), as fast and the decrease against climate perturbations and variations of system parameters.*

Key words: *Interconnection and Damping Assignment Passivity-Based Control (IDA-PBC), Maximum Power Point Tracking (MPPT), Thermoelectric Power Generator, Robust controller system.*

1. Introduction

In the last decade, problems related to energy factors (oil crisis), ecological aspects (climatic change), electric demand (significant growth) and financial/regulatory restrictions of wholesale markets have arisen worldwide. These difficulties, far from finding effective solutions, are continuously increasing, which suggests the need of technological alternatives to ensure their solution. One of these technological alternatives is known as distributed generation (DG), and consists of generating electricity as near as possible of the consumption site, in fact like it was made in the beginnings of the electric industry, but now incorporating the advantages of the modern technology [1]. Here it is consolidated the idea of using clean non-conventional technologies of generation that use renewable energy sources (RESs) that do not cause environmental pollution [2]. The thermoelectric generators (TEG) perfectly fit into this category [3, 4].

The TEGs are solid-state devices engineered to generate electricity directly from heat, what is known

as Seebeck effect [5]. TEGs, which use the thermoelectric or Seebeck effect of semiconductors to convert heat energy to electrical energy, have existed for many years with the initial discovery of the thermoelectric effect being made in 1821 by Thomas J. Seebeck. Due to the relatively low efficiency and high costs associated with the technology it has been limited to specialized military, medical, space and remote applications [6, 7]. However, the recent need to new energy sources at all scales, and the technological development of new generation of power processing devices and circuits, has put the TEG again on the list as viable energy source to be exploited and improved for commercial use, and to diversify its applications [3].

The efficiency changes according to the TE material used in the manufacture of TEGs. In 1995, only materials with maximum efficiency of 5% were available, and after that, new TE materials that provide efficiency greater than 15 % were discovered. Scientists believe that in a near future it is going to be possible to have strongly doped semiconductor materials that have efficiency greater than 25 % [8] and [9].

The output power of the TEG module strongly depends on the temperature gradient applied to the TEG module to maximize the power output of the TEG module, an MPPT algorithm should be used to keep the operating point of the TEG to in the optimum location.

Several MPPT algorithms have been applied for TEG systems, most of these algorithms have been originally developed for photovoltaic (PV) systems [10, 11].

Different methods are used for maximum power point tracking. Currently, Incremental Conduction, Perturb and Observe and Ripple Correlation Control are the most frequently discussed and analysed MPPT

algorithms in literature [12, 13]. All these maximum power point tracking algorithms are rather slow to respond to the fast-changing weather conditions. Furthermore, most of them can not accurately detect the maximum power point [14].

This article develops a method advanced and innovating combining the two techniques (traditional and a nonlinear algorithm of order IDA-PBC) aiming at continuing the maximum power of thermoelectric generator and improved the answers as of traditional algorithm INC already developed, regardless of the change in climatic conditions and system parameters (temperature, load) even in the worst cases. Interconnection and Damping Assignment Passivity-Based Control (IDA-PBC) is a technique that and regulates the behavior of nonlinear systems assigning a desired (Port-Controlled Hamiltonian) structure to the closed-loop [15].

The simulation results showed that the MPPT technique based on passivity (IDA-PBC) present good results and that this controller is powerful and very robust.

This paper is organized as follow, the Thermoelectric Power Generator system and characteristics are discussed in section 2. Section 3 presents the design of the INC MPPT controller. Section 4 presents the Passivity-based control principle. Section 5 presents the design of the proposed IDA-PBC MPPT controller. In section 6, the simulations and result analysis are demonstrated. Also, the comparison analysis between the proposed controller and incremental condition algorithm are provided in this section. In Section 7, we conclude with final remarks.

2. Model Of Thermoelectric Generator

The Thermoelectric module (TEM) is based on the Seeback effect, which states that an electromotive force is introduced between two semiconductors when a temperature difference exists [16].

Several models have been proposed to describe the operation of the thermoelectric module and its behavior under different conditions (temperature gradient and load). The model chosen is the Thevenin Equivalent Circuit of Thermoelectric module (TEM).

This model is known as a Thevenin Equivalent Circuit with voltage source as a function of the temperature gradient and a serial resistance equivalent to the internal resistance. The equivalent electrical diagram of the thermoelectric module as shown in the figure below (Fig. 1).

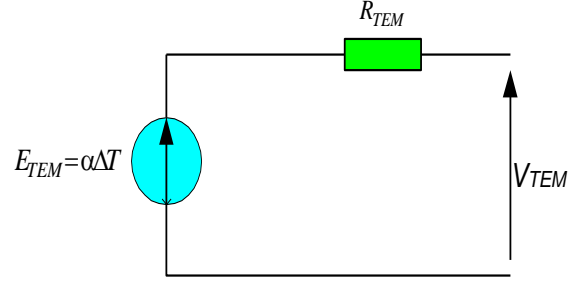


Fig. 1. Diagram electrical equivalent of a Thermoelectric module (TEM) (Thevenin Equivalent Circuit).

where, the TEM electromotive force characteristic of is described by the following expression:

$$E_{TEM} = \alpha_{np} \Delta T \quad (1)$$

E_{TEM} : electromotive force produced by the TEM;

α_{np} : the Seeback coefficients;

ΔT : Temperature gradient;

where, the TEM voltage-current characteristic is described by the following expression:

$$V_{TEM} = \alpha \Delta T - R_s I_{TEM} \quad (2)$$

V_{TEM} : the Output voltage delivered by the TEM;

α_{np} : the Seeback coefficient V/K;

ΔT : the Temperature gradient K;

I_{TEM} : Current produced by the TEM;

R_s : the equivalent serial Resistance of TEM;

A TEG consists of several TEMs, which are electrically connected in a series-parallel arrangement.

The Output voltage V_{TEG} and generated output power are expressed as:

$$V_{TEG} = N_S \alpha \Delta T - R_{TEG} I_{TEG} \quad (3)$$

$$P_{TEG} = N_S N_P V_{TEM} I_{TEM} \quad (4)$$

N_S and N_P : the number of TEMs in series and in parallels.

R_{TEG} : the equivalent serial Resistance of TEG;

V_{TEM} : the Output voltage delivered by the TEG;

I_{TEG} : Current produced by the TEG;

where:

$$R_{TEG} = \frac{N_S}{N_P} R_s \quad (5)$$

$$I_{TEG} = N_P I_{TEM} \quad (6)$$

3. Maximum Power Point Tracking principle (MPPT)

3.1 Principle

The analytical definition of the optimum of a function is the point through which its derivative with respect to a given variable is zero. All algorithms for calculating the maximum power point consulted are based on this principle.

There is an operating point where the power delivered is at a maximum (Fig. 2). The optimization consists in performing this permanently acting automatically on the load seen by the thermoelectric generator, for this adaptation the principle is carried out in general by means of a static converter where the losses should be as low as possible and which can also ensure a shaping according to an outcomes, different attitudes may be considered as to control the adapter.

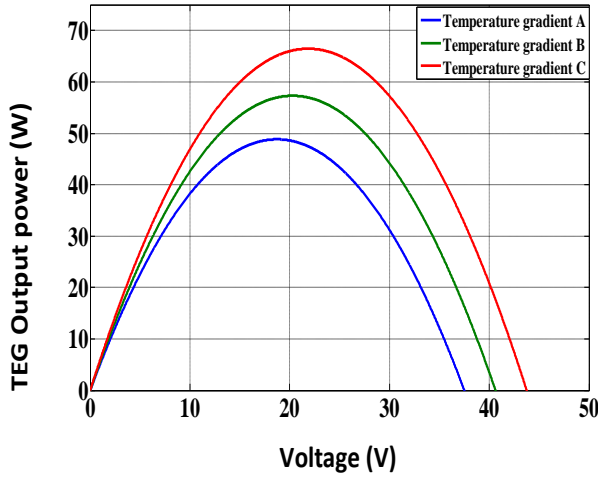


Fig. 2. Characteristic of power delivered by TEG.

This kind of control is often called "Maximum Power Point Search" or "Maximum Power Point Tracking" (MPPT). Fig. 3 shows a basic chain of elementary Power conversion associated with an MPPT control. To simplify the operating conditions of this command, a DC load is chosen friendly. As we can see in this chain, in the case of TEG conversion.

The adapter can be achieved using a DC-DC converter so that the power supplied by the thermoelectric generator corresponds to the maximum power (P_{max}) that generates and it can then be transferred directly to load.

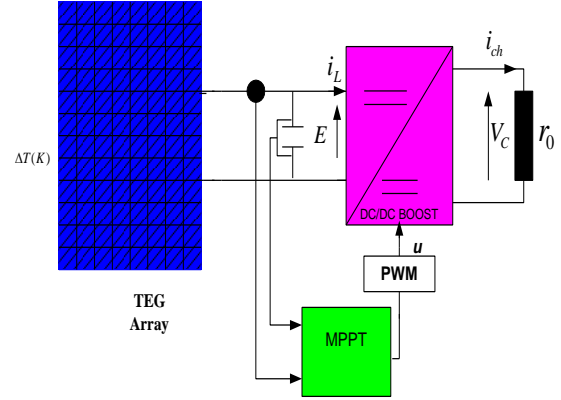


Fig. 3. Schematic diagram of the MPPT converter.

3.2 Incremental Conductance (INC) Algorithm

This algorithm is selected because of its simplicity and the ability to detect and track maximum power point keeping the operation point of solar power plants at it [14].

In this algorithm, calculating the derivative of the panel output power; this derivative is zero at maximum power point, positive and negative to the left to right point MPP [17]. The panel output power P given by: $P = VI$

$$\begin{cases} \frac{dP}{dV} = 0 \Rightarrow P = P_{max} \\ \frac{dP}{dV} < 0 \Rightarrow P < P_{max} \\ \frac{dP}{dV} > 0 \Rightarrow P > P_{max} \end{cases} \quad (7)$$

The partial derivative is $\frac{dP}{dV}$ given by:

$$\frac{dP}{dV} = I + V \frac{dI}{dV} \cong I + V \frac{\Delta I}{\Delta V} \quad (8)$$

Then, (6) can be described as follows:

$$\begin{cases} \frac{\Delta I}{\Delta V} = -\frac{I}{V} \Rightarrow P = P_{max} \\ \frac{\Delta I}{\Delta V} < -\frac{I}{V} \Rightarrow P < P_{max} \\ \frac{\Delta I}{\Delta V} > -\frac{I}{V} \Rightarrow P > P_{max} \end{cases} \quad (9)$$

A flowchart of the INC algorithm is shown in Fig. 4.

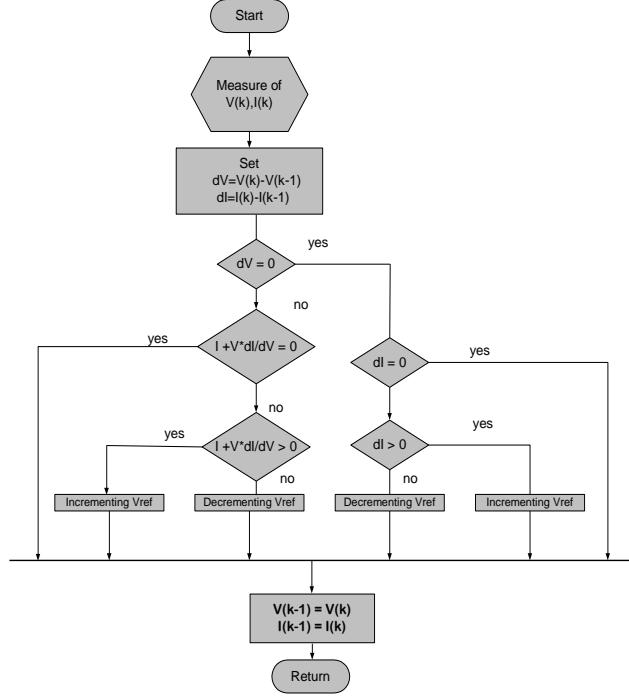


Fig. 4. The flow chart of the INC method.

4. Passivity-Based Control Of Port Controlled Hamiltonian System

4.1 Port controlled Hamiltonian (PCH) System

The Hamiltonian systems modeling formalism controlled port allows the representation of a physical system dynamics as an energy exchange network [18, 19].

A Hamiltonian controlled system (PCH) port on \mathcal{R}^n is defined by an $J(x)$ anti-symmetric structure matrix of dimension $(n \times n)$, $R(x)$ size Diagonal $(n \times n)$, a Hamiltonian function $H(x): \mathcal{R}^n \rightarrow \mathcal{R}$, a matrix of dimension entries $(n \times m)$ and the following dynamic equations:

$$\sum: \begin{cases} \dot{x} = [J(x) - R(x)] \frac{\partial H}{\partial x}(x) + g(x).u \\ y = g^T(x) \frac{\partial H}{\partial x}(x) \end{cases} \quad (10)$$

where $x \in \mathcal{R}^n$ State vector of energy variables.

$H(x): \mathcal{R}^n \rightarrow \mathcal{R}$ Represents the total energy stored.

$u, y \in \mathcal{R}^m$ The (input-output) ports variables powers.

u and y are linear variables, their product is a dual power exchanged with the system environment, eg currents and voltages in electrical circuits.

4.2 Interconnection and Damping Assignment Passivity Based Control (IDA-PBC)

Port Controlled Hamiltonian (PCH) recalling that in the case of internal systems of energy exchanges are captured by the interconnection and damping matrices.

In the first kind, the structure is determining the desired matrices from which the IDA name, after we derive the partial derivative equation (PDE) parameters by the choice of energy matrices.

Finally we choose among all the family which meets the minimum energy and found the control that final convent. The focus IDA-PBC is finding the static controller with feedback loop $u = \beta(x)$.

In closed loop dynamic PCH system with the dissipation of the form:

$$\dot{x} = [J_d(x) - R_d(x)] \frac{\partial H_d}{\partial x}(x) \quad (11)$$

Where the new energy function $H_d(x)$, which will cost a minimum in equilibrium x^* with $J_d(x) = -J_d^T(x)$, and $R_d(x) = R_d^T(x) \geq 0$, are respectively the matrices of interconnections and damping [20].

4.3 IDA-PBC properties

- The energy balance:

The IDA-PBC stabilization mechanism is particularly clear when applied to a PCH system with some suitable damping properties injections. Indeed the natural damping of the PCH system satisfies [21]:

$$R(x)(\nabla H_a - \nabla H) = 0 \quad (12)$$

$R_d(x) = R(x)$ (Along the closed-loop system) the desired energy function is expressed as:

$$H_d(x) = H(x) - \int_0^t u(s).y(s)ds \quad (13)$$

IDA-PBC shows that the energy function is the difference between the energy stored in the system and the energy provided by the environment. This shows that the controller is in energy conservation. Let $J(x, u); R(x); H(x); g(x, u)$ and the desired balance for stability desired.

$x^* \in \mathcal{R}^n$; and functions $\beta(x)$, $J_a(x)$, $R_a(x)$ and the vector $K(x)$

$$\begin{aligned} & [J(x, \beta(x)) + J_a(x) - (R(x) + R_a(x))] \cdot K(x) = \\ & [-J_a(x) - R_a(x)] \frac{\partial H}{\partial x}(x) + g(x, \beta(x)) \end{aligned} \quad (14)$$

- *The structure preservation:*

$$\begin{cases} J_d(x) = J(x, \beta(x)) + J_a(x) = -[J(x, \beta(x)) + J_a(x)]^T \\ R_d(x) = R(x) + R_a(x) = [R(x) + R_a(x)]^T \end{cases} \quad (15)$$

- *Integrability:* $K(x)$ is the gradient of a scalar function.

$$\frac{\partial K}{\partial x}(x) = \left[\frac{\partial K}{\partial x}(x) \right]^T \quad (16)$$

- *The equilibrium assignment:* $K(x)$ to verify in (17):

$$K(x^*) = -\frac{\partial H}{\partial x}(x^*) \quad (17)$$

- *Lyapunov Stability:*

The Jacobian $K(x)$, at x^* satisfies the relationship:

$$\frac{\partial K}{\partial x}(x^*) = -\frac{\partial^2 H}{\partial x^2}(x^*) \quad (18)$$

According to these conditions, the closed loop system becomes a system with a PCH dissipation of the form:

$$\dot{x} = [J_d(x) - R_d(x)] \frac{\partial H_d}{\partial x}(x) \quad (19)$$

where:

$$H_d(x) = H(x) + H_a(x) \quad (20)$$

$$\frac{\partial H_a}{\partial x}(x) = K(x) \quad (21)$$

x^* Becomes a stable equilibrium in a closed loop, it will be asymptotic if we add a great set dynamically closed loop contained in:

$$\left\{ x \in \mathcal{R}^n; \left[\frac{\partial H}{\partial x}(x) \right]^T R_d(x) \frac{\partial H}{\partial x}(x) = 0 \right\} \quad (22)$$

Equal $\{x^*\}$. An estimate of its domain of attraction is given by the largest bounded level set $\{x \in \mathcal{R}^n, H_d(x) \leq c\}$ [22].

4.4 General nonlinear systems

It is considered the form of system

$$\dot{x} = f(x) + g(x).u \quad (23)$$

It is assumed that there are matrices [23]:

$$g^\perp(x); J_a(x) = -J_a^T(x); R_d(x) = R_d^T(x) \geq 0$$

And a function $H_d : \mathcal{R}^n \rightarrow \mathcal{R}$ that checks PDE

$$g^\perp(x).f(x) = g^\perp(x)[J_a(x) - R_d(x)]\nabla H_d \quad (24)$$

where: $g^\perp(x).g(x) = 0$ and $g^\perp(x)$, this is the matrix left $g(x)$ to complete row.

x^* and such that:

$$x^* = \arg \min H_d(x) \quad (25)$$

$x^* \in \mathcal{R}^n$, the stable equilibrium point, therefore the closed loop system with when:

$$\beta(x) = [g^T(x).g(x)]^{-1} g^T(x)[J_d(x) - R_d(x)]\nabla H_d - f(x) \quad (26)$$

PCH takes the form:

$$\dot{x} = [J_d(x) - R_d(x)]\nabla H_d \quad (27)$$

With is a stable equilibrium point (local) can be asymptotically stable if more is a minimum for and represents the largest set invariant under the dynamic closed-loop [24].

$$\{x \in \mathcal{R}^n | [\nabla H]^T R_d(x) \nabla H_d = 0\} \quad (28)$$

Therefore $\{x^*\}$ is given by $\{x \in \mathcal{R}^n | H_d(x) \leq 0\}$.

5. Passivity-based controller design

5.1 Interconnection and Damping Assignment Controller (IDA-PBC) for Boost converter

In this section, we will implement the control law synthesis method based on the passivity of DC-DC converter (Boost). Consider the dynamic model of a thrust power converter that has been depicted in Fig. 5. The converter status equations are:

$$\begin{cases} L \frac{di_L}{dt} = E - (1-u)V_C \\ C \frac{dV_C}{dt} = (1-u)i_L - \frac{V_C}{r_0} \end{cases} \quad (29)$$

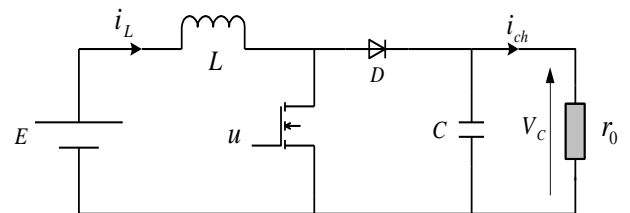


Fig. 5. Schematic Boost Converter.

We can then write, according to the state variables, the energy stored in a capacitor, which plays the role of

the potential energy v_C of the system:

$$v_C = \frac{1}{2C} q_c^2 \quad (30)$$

And the magnetic energy of an inductance, who plays the role kinetic energy T of the system:

$$T = \frac{1}{2L} \Phi_L^2 \quad (31)$$

The Hamiltonian, which represents the total energy of under LC circuit without losses, is then simply:

$$H = T + v_C = \frac{1}{2L} \Phi_L^2 + \frac{1}{2C} q_c^2 \quad (32)$$

Is the state vector: where x_1 is the magnetic flux through the inductor, x_2 is the electric charge in the capacitor.

$$x = \begin{bmatrix} \Phi_L \\ q_C \end{bmatrix} = \begin{bmatrix} Li_L \\ CV_C \end{bmatrix} \quad (33)$$

The Hamiltonian of the system can be written as:

$$H = T + v_C = \frac{1}{2L} \Phi_L^2 + \frac{1}{2C} q_c^2 = \frac{1}{2} x^T Q x \quad (34)$$

with:

$$Q = \begin{bmatrix} \frac{1}{L} & 0 \\ 0 & \frac{1}{C} \end{bmatrix} \quad (35)$$

Thus deriving the Hamiltonian with respect to the state vector, we get:

$$\frac{\partial H(x)}{\partial x} = Qx = \begin{bmatrix} \frac{\Phi_L}{L} \\ \frac{q_c}{C} \end{bmatrix} = \begin{bmatrix} i_L \\ V_C \end{bmatrix} \quad (36)$$

This leads to model state:

$$\dot{x} = \begin{bmatrix} 0 & 1-u \\ u-1 & -\frac{1}{r_0} \end{bmatrix} \frac{\partial H}{\partial x} + \begin{bmatrix} 1 \\ 0 \end{bmatrix} E \quad (37)$$

This model can be written in the simplified form:

$$\dot{x} = (J - R) \frac{\partial H}{\partial x} + g(x) E \quad (38)$$

where we have the matrices:

$$J = \begin{bmatrix} 0 & u-1 \\ 1-u & 0 \end{bmatrix} \text{ anti-symmetric, } R = \begin{bmatrix} 0 & 0 \\ 0 & \frac{1}{r_0} \end{bmatrix},$$

$$g(x) = \begin{bmatrix} 1 \\ 0 \end{bmatrix}, R_a = \begin{bmatrix} r_a & 0 \\ 0 & -\frac{1}{r_0} \end{bmatrix}, R_d = \begin{bmatrix} r_a & 0 \\ 0 & 0 \end{bmatrix}.$$

we have:

$$R_d = R + R_a \text{ with: } \begin{cases} R_d(x) = R(x) + R_a(x) \\ J_d(x) = J(x, u) + J_a(x) \end{cases}$$

The balance points to the desired voltage capacitor items are indicated by $x_d = [x_{1d} \ x_{2d}]^T$.

with: $x_{1d} = LV_d^2 / r_0 E$, $x_{2d} = CV_d$ and $u_d = 1 - \frac{E}{V_d}$.

Pause u is based on independent and x_1 to $x_2 : u = \beta(x_2)$, and $J_a(x) = 0$, Taking:

$$K(x) = [K_1 \ K_2]^T = \frac{\partial H_a}{\partial x} \quad (39)$$

So the desired total energy: $H_d = H_a + H$

$$(J(\beta(x)) - R_d) \frac{\partial H_a}{\partial x} = R_a \frac{\partial H}{\partial x} + g(x) E \quad (40)$$

This leads to we get the system of equations:

$$\begin{bmatrix} -r_a & u-1 \\ 1-u & 0 \end{bmatrix} \begin{bmatrix} K_1 \\ K_2 \end{bmatrix} = \begin{bmatrix} r_a & 0 \\ 0 & -\frac{1}{r_0} \end{bmatrix} \begin{bmatrix} \frac{1}{L} x_1 \\ \frac{1}{C} x_2 \end{bmatrix} + \begin{bmatrix} 1 \\ 0 \end{bmatrix} E \quad (41)$$

By solving the system of (41) with K_1 and K_2 are unknown which gives :

$$K = \begin{bmatrix} K_1 \\ K_2 \end{bmatrix} = \begin{bmatrix} -\frac{x_2}{r_0 C (1 - \beta(x_2))} \\ \frac{R_a x_2}{r_0 C (1 - \beta(x_2))^2} - \frac{r_a x_1 / L + E}{1 - \beta(x_2)} \end{bmatrix} \quad (42)$$

we have:

$$\frac{\partial K_1(x)}{\partial x_2} = \frac{\partial K_2(x)}{\partial x_1} \quad (43)$$

we find :

$$-\frac{r_a}{L(1 - \beta(x_2))} = -\left(\frac{x_2}{r_0 C (1 - \beta(x_2))^2} \frac{d\beta(x_2)}{dx_2} \right) - \frac{1}{r_0 C (1 - \beta(x_2))} \quad (44)$$

Therefore:

$$\frac{x_2}{1 - \beta(x_2)} \frac{d\beta(x_2)}{dx_2} = -(1 - \frac{Cr_a r_0}{L}) \quad (45)$$

The two variables are separated:

$$\frac{d\beta(x_2)}{1-\beta(x_2)} = -\left(1 - \frac{Cr_a r_0}{L}\right) \frac{dx_2}{x_2} \quad (46)$$

The both terms of equality is integrated:

$$\int \frac{d\beta(x_2)}{1-\beta(x_2)} = -\left(1 - \frac{Cr_a r_0}{L}\right) \int \frac{1}{x_2} dx_2 \quad (47)$$

Defining $\alpha = 1 - (Cr_a r_0)/L$, The controller will be:

$$u = \beta(x_2) = 1 - c_1 x^\alpha \quad (48)$$

where c_1 is constant calculated by the equation:

$$\left. \frac{\partial H_d(x)}{\partial x} \right|_{x=x_2} = \left(\frac{\partial H}{\partial x} + \frac{\partial H_a}{\partial x} \right) \bigg|_{x=x_2} = 0 \quad (49)$$

result:

$$c_1 = (1 - u_d) / (CV_d)^\alpha \quad (50)$$

This gives a non-linear IDA-PBC control law of the form:

$$u = 1 - (1 - u_d) (x_2 / x_{2d})^\alpha \quad (51)$$

The proposed nonlinear controller ensures the stability and fast response of the system during large disturbances in load and DC-bus voltage [25].

5.2 Design of MPPT Controller based on Passivity

The control objective is to maximize the power extracted from a TE generating system, In order to combine the MPPT with passivity based control reasonably, considering the operating power point of TEG array can be controlled by adjusting of the inverter (Boost) output voltage to tracking a desired V_d by using the IDA-PBC controller design of (51) where the INC algorithm provides the reference voltage V_d for developed the desired power output . with :

$$V_d = (1 - u) V_{TEGMPPT} \quad (52)$$

In summary the block diagram of Passivity-based control for maximum power extraction of thermoelectric generator system in shown in Fig. 6

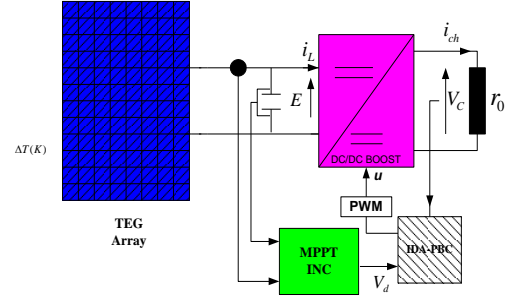


Fig. 6. Overall control loop for TEG system.

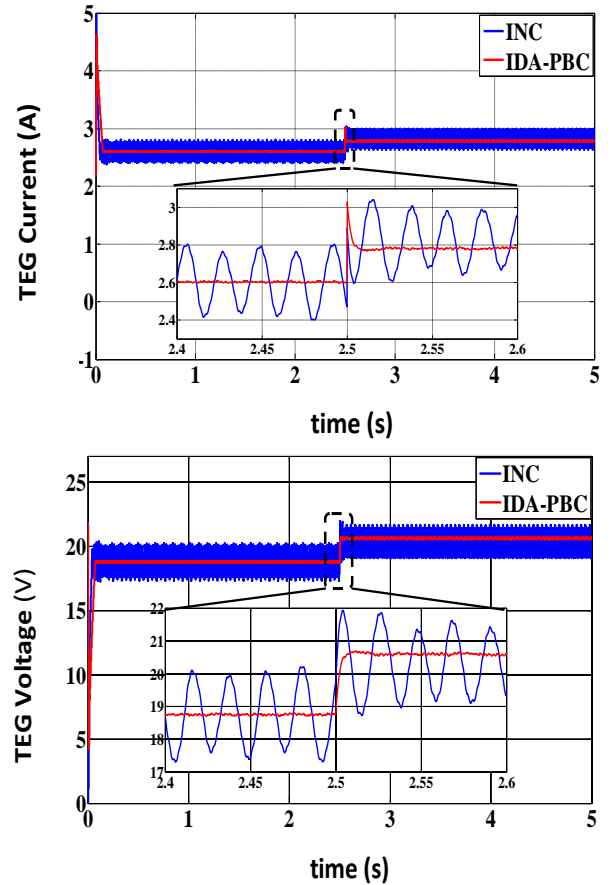
6. Simulation results and discussion

6.1 Robustness study of INC and IDA-PBC applied for TEG system

To validate the algorithm operation INC MPP and IDA-PBC MPP the TEG, is performed by introducing variations on the different intervening variables on the operational MPPT. Furthermore, ranks for some variables in $t = 2.5s$, is introduced.

-Temperature gradient variation

Assuming a rise in temperature gradient from $60^\circ C$ to $65^\circ C$ at time $t = 2.5$ sec, the simulation results are shown in Fig. 7.



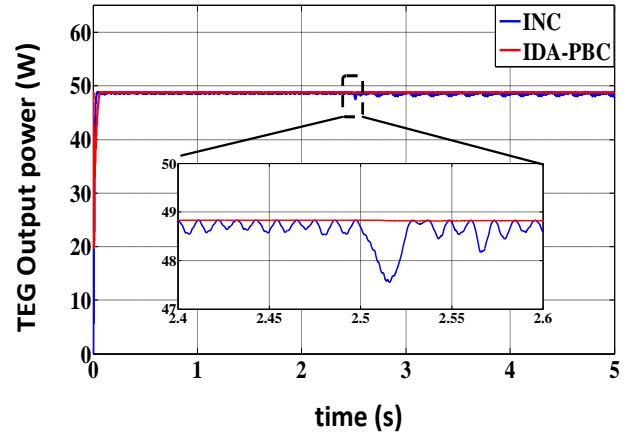
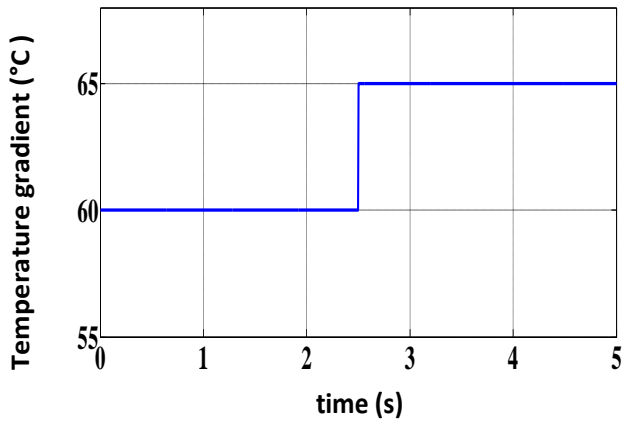
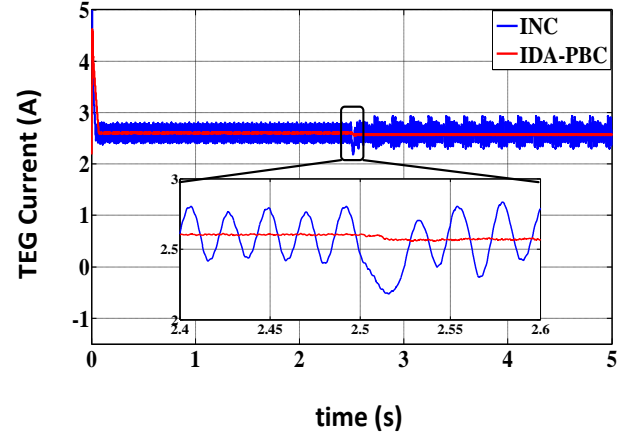
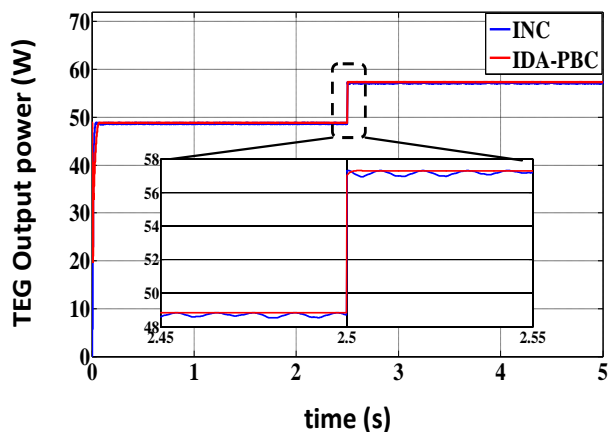


Fig. 7. Outcomes INC MPPT algorithms and IDA-PBC MPPT for a temperature gradient increase of 60°C to 65°C whit load 10 Ohm

-Load variation

Assuming a load increase from 10 to 20 Ohm at time $t = 2.5$ simulation results are shown in Fig. 8.

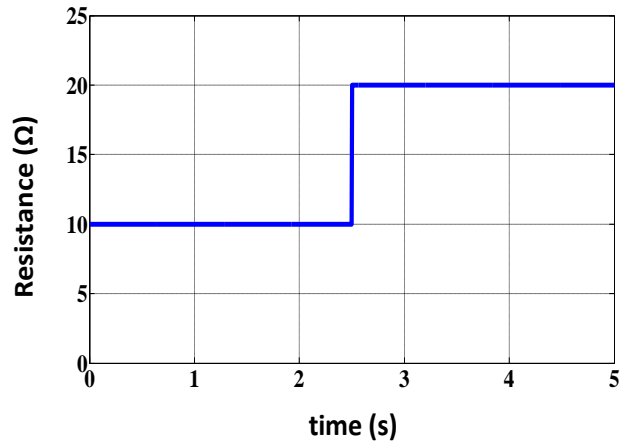
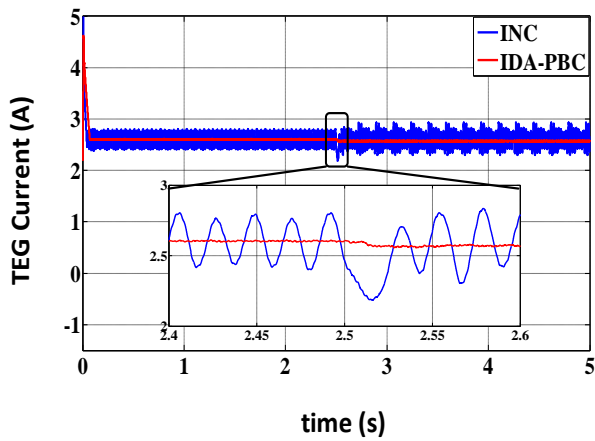


Fig. 8. Responses INC and IDA-PBC algorithms for load increase 10 to 20 Ohm with temperature gradient 60°C

-Temperature gradient and load changes

Here, it's exposed both MPPT algorithms to a change in various parameters temperature gradient and the load at the same time, simulation results are shown in Fig. 9.

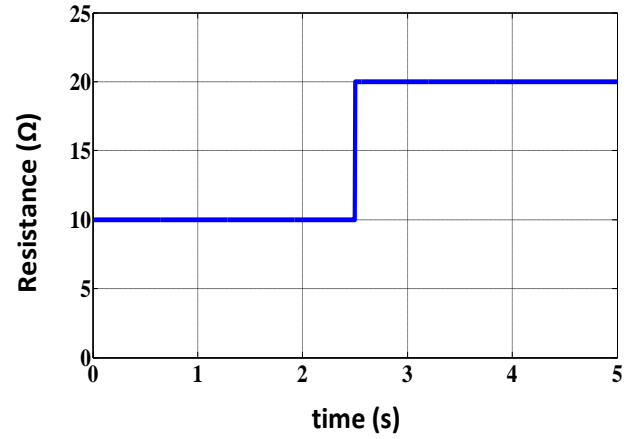
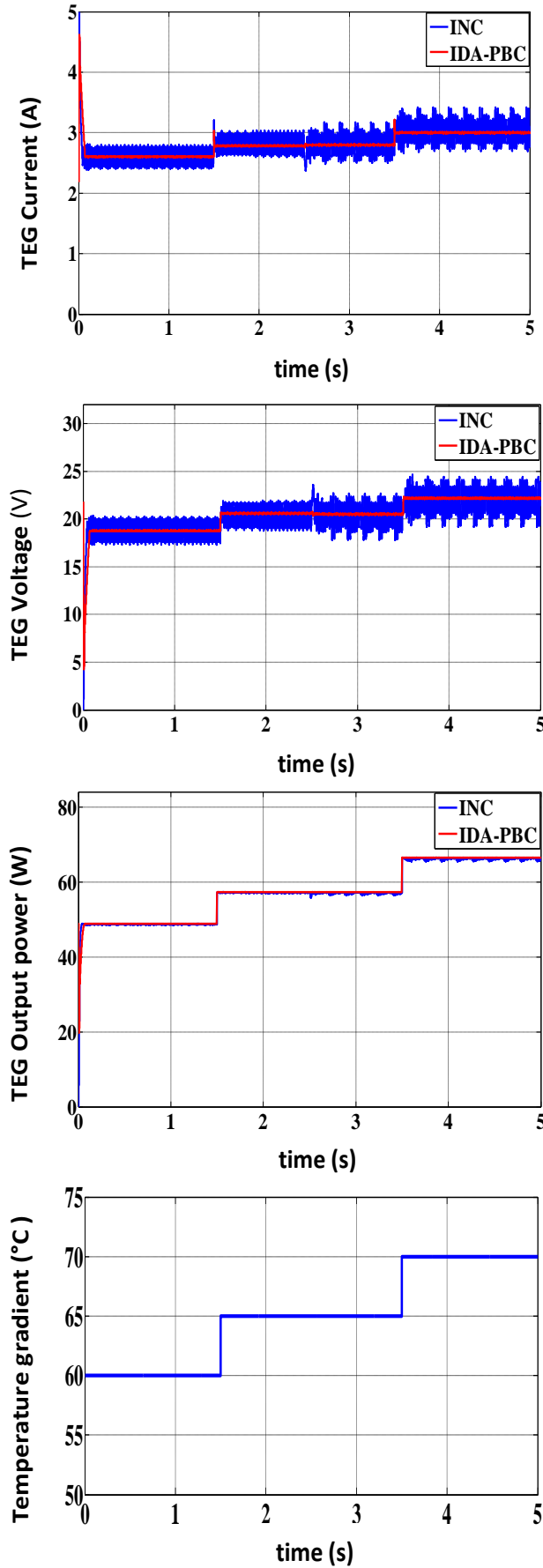


Fig. 9. Outcomes of MPPT algorithms INC and IDA-PBC achievement for a parameters variations.

6.2 Discussion of the results

In Fig. 7 shows the effect of increasing in power, caused by an increase of the temperature gradient, which causes a deviation of the maximum power point MPP for both algorithms with increased current and voltage. Once the temperature gradient stabilizes, the power returns to its steady state with less disruption to IDA-PBC MPPT. This has resulted a very short response time and better dynamic performance with negligible disruption over INC MPPT.

It's also noted that in Fig. 8, despite the change in the load, both MPPT algorithms have retained the optimal values of the power of TEG generator, and negligible disruption to IDA-PBC MPPT, consequently a good income.

In Fig. 9 shows the performance of two algorithms in the case of variation in temperature gradient and load the results of this test show the good pursuit of both algorithms but with speed and higher steadiness and less disruption as of IDA-PBC MPPT controller responses compared to INC MPPT controller.

7. Conclusion

In this paper, a new MPPT control method was proposed for a thermoelectric generator system. The MPPT control method was employed with the aim to harvest the maximum power from TE generator power. The control method was presented based on Interconnection and Damping Assignment Passivity Based Control (IDA-PBC), directly creating the control signal for handling the power electronic converter, shows its efficiency and robustness to the other proposed control (INC method) as the speed and lower disturbances against climate change as well as system settings.

References

1. Willis HL, Scott WG. *Distributed power generation – planning and evaluation*. 1st ed. Marcel Dekker, ISBN 0-8247-0336-7;2000.
2. Rahman S. Going green: the growth of renewable energy. *IEEE Power and Energy Magazine* Nov/Dec 2003;1(6):16–8
3. D. Rowe, "Thermoelectric waste heat recovery as a renewable energy source," *Int. J. Innov. Energy Syst. Power*, vol. 1, pp. 13-23, 2006.
4. Z. M. Dalala and Z. U. Zahid, "New MPPT algorithm based on indirect open circuit voltage and short circuit current detection for thermoelectric generators," in *Energy Conversion Congress and Exposition (ECCE)*, 2015 IEEE, 2015, pp. 1062-1067.
5. S. B. Riffat and X. Ma, "Thermoelectrics: a review of present and potential applications," *Applied Thermal Engineering*, vol. 23, pp. 913-935, 2003.
6. D. Rowe, "Thermoelectrics, an environmentally-friendly source of electrical power," *Renewable Energy*, vol. 16, pp.1251-1256, 1999.
7. N. Phillip, O. Maganga, K. J. Burnham, J. Dunn, C. Rouaud, M. A. Ellis, and S. Robinson, "Modelling and simulation of a thermoelectric generator for waste heat energy recovery in Low Carbon Vehicles," in *Environment.Friendly Energies and Applications (EFEA)*, 2012 2nd International Symposium on, 2012, pp. 94-99.
8. T. Hendricks and W.T. Choate, "Engineering Scoping Study of Thermoelectric Generator Systems for Industrial Waste Heat Recovery," *Pacific Northwest National Laboratory*, 2006.
9. A.E.S.S. Fernandes, " *Conversão de energia com células de Peltier*. Dissertação (Mestrado), "Lisboa: Universidade Nova de Lisboa, 2012.
10. N. Kasa, T. Iida, and C. Liang, "Flyback Inverter Controlled by Sensorless Current MPPT for Photovoltaic Power System," *Industrial Electronics, IEEE Transactions on*, vol.52, pp. 1145-1152, 2005.
11. K. Rae-young and L. Jih-Sheng, "A Seamless Mode Transfer Maximum Power Point Tracking Controller For Thermoelectric Generator Applications," *Power Electronics, IEEE Transactions on*, vol. 23, pp. 2310-2318, 2008.
12. T. Eswam, P.L. Chapman, "Comparison of photovoltaic array maximum power point Tracking methods," *IEEE Transactions on Energy Conversion*, Vol. 22, No. 2, June 2007.
13. A. Dolara, R. Faranda, S. Leva, *Energy Comparison of Seven MPPT Techniques for PV Systems*, *J. Electromagnetic Analysis & Applications*, vol. 3, pp. 152–162, Sept. 2009.
14. M. Pikutis, D. Vasarevicius, R. Martavicius, *Maximum Power Point Tracking in Solar Power Plants under Partially Shaded Condition*, *Elektronika ir Elektrotechnika*, vol. 20, no. 4, pp. 49–52, 2014.
15. R. Ortega and E. Garcia–Canseco, *Interconnection and Damping Assignment Passivity–Based Control: Towards a Constructive Procedure—Part I*, 43rd IEEE Conference on Decision and Control pp. 3412–3417, December, 2004.
16. S. Lineykin and S. Ben-yaakov, "Modeling and analysis of thermoelectric modules," *IEEE Trans. Ind. Appl.*, vol. 43, no. 2, pp. 505–512, Mar./Apr. 2007.
17. J. RL, P.A, H.C.RL, D. RAJA, "Simulation of incremental conductance mppt with direct control and fuzzy logic methods using SEPIC converter," *Journal of Electrical Engineering*, Vol 13, no. 3, pp. 91-99, 2013.
18. M. Miguel Magos rivera, *la modélisation des systèmes dynamiques à topologie variable : une formulation Hamiltonienne à ports paramétrée*, Ph.D. thesis, University of Claud Bernard–Lyon1, 2005.
19. H. Gonzalez, M.A. Duarte-Mermoud, I. Pelissier, *A novel induction motor control scheme using IDA-PBC*, University of Chile, Casilla 412-3, Santiago, Chile, 2008.
20. R. Ortega, A. van der Schaft, B. Maschke, et al, *Interconnection and damping assignment passivity-based control of port-controlled Hamiltonian systems*, *Automatica*, vol. 38, no. 4, pp. 585-596, 2002.
21. B.M. Maschke, A.J. Van der Schaft, *Hamiltonian Formulation of Distributed-Parameter Systems with Boundary Energy Flow*, *Journal of Geometry and Physics*, pp.166-174.2002.
22. A. Doria-cerezo, *modeling simulation and control of doubly-fed induction machine controlled by a back-to-back converter*, thesis doctorate, universitat politècnica de Catalunya, juliol Del 2006.
23. Z. Wang P. Goldsmith, *Modified energy-balancing-based control for the tracking problem*, *IET Control Theory Appl.*, vol. 2, no. 4, pp. 310–322, 2008.
24. J.A. Acosta, R. Ortega and Astol, *interconnection and damping assignment passivity-based control of mechanical systems with underactuation degree one*, American control conference, Boston, USA, June 30, July 2, 2004.
25. J. Zeng, Z. Zhang and W. Qiao, *An interconnection-damping-assignment passivity-based controller for a DC-DC boost converter with a constant power load*, *IEEE Industry Applications Society Annual Meeting*, Las Vegas, NV, pp. 1-7, 2012.